Penerbit Akademia Baru

Journal of Advanced Research in Fluid Mechanics and Thermal Sciences

Journal homepage: www.akademiabaru.com/arfmts.html
ISSN: 2289-7879

Computational Investigations of Arrhenius Activation Energy and Entropy Generation in A Viscoelastic Nanofluid Flow Thin Film Sprayed on A Stretching Cylinder

Auwalu Hamisu Usman[1,4], Noor Saeed Khan[2,3,5], Sadiya Ali Rano[4], Usa Wannasingha Humphries[1,*], Poom Kumam[3,5,♣]

[1] Department of Mathematics, Faculty of Science, King Mongkut's University of Technology Thonburi (KMUTT), 126 Pracha-Uthit Road, Bang Mod, Thung Khru, Bangkok 10140, Thailand
[2] Department of Mathematics, Division of Science and Technology, University of Education, Lahore 54000, Pakistan
[3] KMUTTFixed Point Research Laboratory, Room SCL 802 Fixed Point Laboratory, Science Laboratory Building, Department of Mathematics, Faculty of Science, King Mongkut's University of Technology Thonburi (KMUTT), 126 Pracha-Uthit Road, Bang Mod, Thung Khru, Bangkok 10140, Thailand
[4] Department of Mathematical Science, Faculty of Physical Sciences, Bayero University Kano – 700241, Kano, Nigeria
[5] Center of Excellence in Theoretical and Computational Science (TaCS-CoE), Science Laboratory Building, Faculty of Science, King Mongkut's University of Technology Thonburi (KMUTT), 126 Pracha-Uthit Road, Bang Mod, Thung Khru, Bangkok 10140, Thailand

ARTICLE INFO

Article history:
Received 4 April 2021
Received in revised form 22 June 2021
Accepted 2 July 2021
Available online 12 August 2021

Keywords:
Arrhenius activation energy; Binary chemical reaction; Entropy generation; Film spray; HAM; Viscoelastic nanofluid

ABSTRACT

This paper investigates the two-dimensional and incompressible flow of viscoelastic nano-liquid dynamic and axisymmetric sprayed thin film deposit on a stretched cylinder. It also looked at how activation energy and entropy evaluation affected mass and heat flow. The governing equations are transformed into nonlinear ordinary differential equations using similarity transformation techniques, which are then resolved successively using a strong semi analytical homotopy analysis method (HAM). The velocity decreases as the magnetic field strength and viscoelastic parameters are increased. The temperature rises as the Brownian motion parameter increases, while it falls as the Prandtl number, film thickness parameter, and thermophoresis parameter increase. The greater the Reynolds number and the activation energy parameter, the higher the concentration of nanoparticles. The film size increases nonlinearly with the spray rate. Entropy generation increases as the Brinkmann number, magnetic field, and thermal radiation parameters increase. A nearby agreement is signed after comparing current investigation with published results. The results obtained, possibly under ideal conditions, could be useful for determining and architecting coating applications.

* *Corresponding author.*
E-mail address: usa.wan@kmutt.ac.th
♣ *Corresponding author.*
E-mail address: poom.kum@kmutt.ac.th

https://doi.org/10.37934/arfmts.86.1.2751

1. Introduction

Non-Newtonian fluid advancement is critical for new developments and productions in many industrial sectors. The application of magnetic hydrodynamics to electrically conductive fluids is directly related to the results that can be obtained by linking any external magnetic field current and fluid momentum. Some non-Newtonian main applications investigated and reported by Albano *et al.,* [1] include metallurgy (form control, homogenization, sample levitation material), molten steel flow, planetary science and astrophysics, and fusion reactors. The viscoelastic fluid model is essential for the type of fluid due to its remarkable behavior. Han *et al.,* [2] studied viscoelastic fluids in conjunction with the Cattaneo–Christov heat flux model. Mrokowska and Krzto-Maziopa [3] investigated the viscoelastic and shear-thinning effects of an aqueous exopolymer solution on the disk and sphere. Li *et al.,* [4] investigated MHD viscoelastic flow and heat transfer through a vertical stretching sheet with Cattaneo-Christov heat flow effects. There are studies that provide more information on Newtonian and non-Newtonian fluids [5-11].

Liquid cooling is improved by nano-sized particles with diameters ranging from 1 to 100 nm. These nanoparticles are mixed with the base fluid, which improves cooling by having a higher coefficient of heat transfer than normal liquids, this mixture is known as a nanofluid. Choi and Bestman [12] pioneered the concept of nanofluids at the Argonne National Laboratory in the United States. Nanotechnology is currently one of the most fascinating fields. It is frequently a special type of fluid with greater thermal conductivity than standard host fluids. Buongiorno [13] evaluated Brownian motion and thermophoretic features to determine the convective transport of nanoparticles. Chakraborty and Panigrahi [14] investigated and review the stability of nanofluid. Ellahi *et al.,* [15] investigated the heated couple stress bi-phase fluid with spherical Hafnium particles metal. The flow bounded by two parallel plates in the paper is entirely caused by the influence of an axial pressure gradient. There are studies that provide more information about the recent studies on nanofluids [16-25].

Thin film flow is regarded as a significant area of research. Thin film fluids are used to make a variety of heat exchangers and chemical tools; however, these technologies necessitate a thorough understanding of the movement process. Among the numerous applications for thin film fluids were wire and fiber coating, polymer preparation, and other applications for thin film fluids. This motion is associated with the production of various types of sheets, whether metal or plastic. In recent years, some researchers have considered working on this type of flow. Ellahi *et al.,* [26] studied the thin film coating on the multi-fluid flow of a rotating disk suspended with nano-size silver and gold particles. Further researches can be found in others studies [27-29].

The species does not normally respond to chemical reactions with Arrhenius activation energy, which is one of the most significant indicators. Arrhenius [30] was the first to investigate the term activation energy. The minimum energy required for the process of molecules or atoms in chemical reactions, on the other hand, is referred to as activation energy. Bestman [31] may have described a principal model that consists of a boundary layer of fluid flow problems caused by binary chemical reactions with Arrhenius activation energy for perhaps the first time. The flow of a binary chemical reacting fluid with Arrhenius activating energy and convective boundary conditions is the focus. One of several goals of this study is to see how activation energy affects fluid flow and binary chemical reactions. More such research is available in the other studies [32-36].

It has been observed that when a cylinder is stretched, adequate attention is given to the stretching of the cylinder's flow. Wang [37] was the first to investigate the steady-state incompressible viscous fluid across the expanding cylinder. Bachok and Ishak [38] examined and

found on the stretching cylinder's numerical flow and thermal transfer solution. Further research is available in the other studies [39-44].

This research paper is supplemented by a number of intriguing studies on stretching cylinders in the literature. To the best of knowledge, no investigation into the core problems has taken place. This paper investigates the steady two-dimensional, incompressible radiative flow of the viscoelastic nanofluid and axisymmetric sprayed thin film deposition past the stretching cylinder while accounting for the effect of activation energy and entropy measured. The fluid flow problem is governed by partial differential equations, which are transformed into ordinary differential equations through the use of appropriate similarity transformations. Liao introduced HAM for the first time in 1992 [45-47]. The solution of this method is fast convergent. Due to its rapid convergence, various researchers such as Usman *et al.,* [48] and Shah *et al.,* [49] have used HAM to solve their fluid flow problems. The results obtained for the effects of all related parameters on all profiles are graphically presented.

2. Problem Formulation

At $r = 0$, the steady, two-dimensional, and incompressible flow of viscoelastic and axisymmetric sprayed thin film nanofluid is considered. $r > 0$, consider to be the domain of the flow and $z - axis$ is consider to be the axis of cylinder and $r - axis$ is consider to be the radial direction. The effects of the magnetic field are used in the radial direction. Suggesting that the effects of induced magnetic fields are negligible. A radial axisymmetric spray with velocity V condenses as a film and is drawn along the cylinder's outer surface, see Figure 1. Let T and C represent the fluid temperature and nanoparticles concentration respectively. At the outer radius b of the film thickness with β_1 as the nondimensional film thickness parameter, T_b temperature at the outer radius of the film surface, T_w temperature at the wall, C_w Nanoparticle concentration at the wall, C_b Nanoparticle concentration beyond the surface , T_{ref} is the reference temperature, C_{ref} reference concentration, c, a are constants.

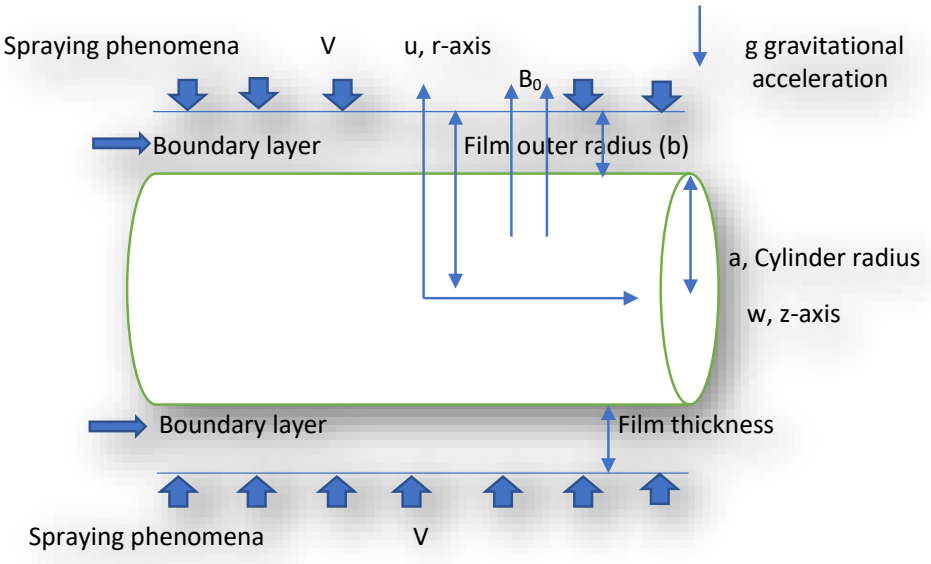

Fig. 1. Geometry of the Problem

The fluid flow governing equations that have been modelled are [11,27,37-39]

$$\frac{\partial u}{\partial r}+\frac{u}{r}+\frac{\partial w}{\partial z}=0, \tag{1}$$

$$u\frac{\partial w}{\partial r}+w\frac{\partial w}{\partial z}=\nu\left[\frac{\partial^2 w}{\partial r^2}+\frac{1}{r}\frac{\partial w}{\partial r}\right]-\frac{\sigma B_o^2 w}{\rho_f}+\frac{k_o}{\rho_f}\left[\begin{array}{l} w\frac{\partial^3 w}{\partial r^3}+w\frac{\partial^3 w}{\partial z\partial r^2}-\frac{\partial w}{\partial r}\frac{\partial^2 u}{\partial r^2}+\frac{\partial w}{\partial z}\frac{\partial^2 w}{\partial r^2}+ \\ \frac{1}{r}\left(u\frac{\partial^2 w}{\partial r^2}+w\frac{\partial^2 w}{\partial z\partial r}-\frac{\partial u}{\partial r}\frac{\partial w}{\partial r}+\frac{\partial w}{\partial z}\frac{\partial w}{\partial r}\right) \end{array}\right]+ \tag{2}$$

$$\frac{1}{\rho_f}\left[(1-C_b)\rho_f\beta^*(T-T_b)-(\rho_p-\rho_f)(C-C_b)\right]g$$

$$u\frac{\partial T}{\partial r}+w\frac{\partial T}{\partial z}=\alpha_1\left[\frac{\partial^2 T}{\partial r^2}+\frac{1}{r}\frac{\partial T}{\partial r}\right]+\tau\left[D_B\frac{\partial C}{\partial r}\frac{\partial T}{\partial r}+\frac{D_T}{T_b}\left(\frac{\partial T}{\partial r}\right)^2\right]-\frac{1}{(\rho c_p)_f}\frac{\partial (rq_r)}{\partial r} \tag{3}$$

$$u\frac{\partial C}{\partial r}+w\frac{\partial C}{\partial z}=D_B\frac{1}{r}\frac{\partial}{\partial r}\left(r\frac{\partial C}{\partial r}\right)+\frac{D_T}{T_b}\frac{1}{r}\frac{\partial}{\partial r}\left(r\frac{\partial T}{\partial r}\right)-k_r^2(C-C_b)\left(\frac{T}{T_b}\right)^n\exp\left[\frac{-E_a}{kT}\right] \tag{4}$$

with boundary conditions

$$w(z,r)=W_w(z),\ \ u(z,r)=U_w(z),\ \ T(z,r)=T_w(z),\mathrm{C}(z,r)=C_w(z)\ \text{at}\ r=a, \tag{5}$$

$$\frac{\partial w}{\partial r}=0,\frac{\partial \delta}{\partial r}=0,\frac{\partial C}{\partial r}=0,\frac{\partial T}{\partial r}=0,\ u=\frac{\partial \delta}{\partial z}\ \text{at}\ r=b \tag{6}$$

where δ is the film size, B_o is the magnetic field strength, σ is the electrical conductivity, k_0 is the relaxation time coefficients, g is the gravity acceleration, ρ_p stands for the liquid density, ν_f is the kinematic viscosity, μ dynamic viscosity, u and w are velocity components, the nanoparticles volume is C, the fluid temperature is T, ρ_f is the density of base fluid, α_1 is the thermal diffusivity, D_B is the Brownian motion, D_T is the thermophoretic diffusion coefficient, and the heat capacity ratio is τ.

According to the Rosseland approximation the thermally developed flow can be expressed as a modification with σ^{**} is represented as Stefan-Boltzmann constant and k^{**} as the mean absorption coefficient [8].

$$q_r=-\frac{16\sigma^{**}T_b^3}{3k^{**}}\frac{\partial T}{\partial r}\ , \tag{7}$$

Introducing the transformation for non-dimensionless functions f,θ,ϕ and similarity variable ζ as [27]

$$\zeta = \left(\frac{r}{a}\right)^2, u = -ca\frac{f(\zeta)}{\sqrt{\zeta}}, w = 2czf'(\zeta), T(z) = T_b - T_{ref}\left[\frac{cz^2}{\nu_{\eta f}}\right]\theta(\zeta), \mathrm{C}(z) = C_b - C_{ref}\left[\frac{cz^2}{\nu_{\eta f}}\right]\phi(\zeta). \tag{8}$$

$$\zeta = \left(\frac{b}{a}\right)^2 = \beta_1, \tag{9}$$

Eq. (1) is satisfied through Eq. (8) whereas Eq. (2)-(6) have the following form

$$\frac{1}{\mathrm{Re}}(2f''+2\zeta f''')-Mf'+ff''-f'^2+\lambda_1\left(4ff'f''+\frac{1}{\zeta}f^2f''-2f^2f'''-2Mff''\right)+ \\ -Gr\theta+Gm\phi=0 \tag{10}$$

$$(1+Rd)(2\theta'+\zeta\theta'')-Nb\phi'\theta'-Nt\theta'^2+Pr(f\theta'-2f'\theta)=0 \tag{11}$$

$$Sc(\phi'+\zeta\phi'')+f\phi'-2f'\phi+\frac{Nt}{Nb}(\theta'+\zeta\theta'')-\gamma_1(\gamma_2-\theta_w\theta)^n e^{-\left[\frac{E}{(\gamma_2-\theta_w\theta)}\right]}=0 \tag{12}$$

with boundary conditions given by

$$\begin{aligned} &f = f' = \theta = \phi = 1 \ \ at \ \varsigma = 1 \\ &f'' = \theta' = \phi' = 0 \ \ at \ \varsigma = \beta_1 \end{aligned} \tag{13}$$

where Gr is the thermal Grashof number, Gm is the solutal Grashof number, Re is Reynolds number, M is the parameter of the magnetic field, Pr is the Prandtl number, Nt is the parameter of thermophoresis, Nb is the parameter of Brownian motion, Sc is the Schmidt number, Rd is the radiation parameter, λ_1 is the viscoelastic parameter, γ_1 is chemical reaction rate constant, γ_2 is the temperature ratio, θ_w is dimensionless wall temperature, E is the activation energy parameter, are defined as:

$$\begin{aligned} &\mathrm{Re} = \frac{ca^2}{\nu_f}, M = \frac{\sigma B_0^2}{2c\rho_f}, \lambda_1 = \frac{k_0 c}{\rho_f}, Gr = \frac{g\beta^*(1-C_b)(T_w-T_b)}{4c^2a}, Gm = \frac{g(\rho_p-\rho_f)(C_w-C_b)}{4c^2\rho_f a}, Rd = \frac{32\sigma^{**}T_\infty^3}{3(\rho c)_f k^{**}\alpha_1}, \\ &Nb = \frac{\tau D_B(C_w-C_b)}{\alpha_1}, Nt = \frac{\tau D_T(T_w-T_b)}{\alpha_1}, Sc = \frac{2D_B}{ca^2}, \gamma_1 = \frac{k_r^2}{2c}, \gamma_2 = \frac{T_w}{T_b}, \theta_w = \frac{T_w-T_b}{T_b}, E = \frac{E_a}{kT_b}, \mathrm{Pr} = \frac{\mu c_p}{k} \end{aligned} \tag{14}$$

The shear stress on the surface of the outer film is zero i.e., $f''(\beta_1)=0$. And the shear stress on the cylinder is

$$\tau = \frac{\rho_f \nu_f 4czf''(1)}{a} = \frac{4cz\mu_f f''(1)}{a} \tag{15}$$

The deposition velocity V in terms of film thickness β_1, Mass flux m_1 (interesting quantity which in connection with the deposition per axial length) and normalized mass flux m_2 are given respectively

$$ca\frac{f(\beta_1)}{\sqrt{\beta_1}}=V, m_1=2\pi bV \text{ and } m_2=\frac{m_1}{2\pi a^2 c}=\frac{m_1}{4\pi v_f \operatorname{Re}}=f(\beta_1) \tag{16}$$

3. Physical Quantities

The physical quantities of interests which estimate the skin friction coefficient (C_f), heat transfer coefficient (Nu) and mass transfer coefficient (Sh) which are very important through the industrial application point of view are also calculated in this study. The equation defining the skin friction is

$$C_f=\frac{2\tau_{rz}}{\rho_f (W_w)^2}|_{r=a} \text{ with } \tau_{rz}=\mu_f\left(\frac{\partial w}{\partial r}-k_o w\right)_{r=a}$$
$$C_f=\frac{2}{\operatorname{Re}_z^{\frac{1}{2}}}\left(f''(1)+\frac{f'(0)}{\lambda_1}\right) \tag{17}$$

The equation defining the heat transfer is

$$Nu=\left(\frac{aq_h}{k(T_w-T_b)}\right)|_{r=a} \text{ with } q_h=\left(-k\frac{\partial T}{\partial r}+q_r\right)|_{r=a},$$
$$Nu=-(2+\mathrm{Rd})\theta'(1) \tag{18}$$

The equation defining the mass transfer is

$$Sh=\frac{aq_m}{D_B(C_w-C_b)}|_{r=a} \text{ with } q_m=-D_B\frac{\partial C}{\partial r}|_{r=a},$$
$$Sh=-2\phi'(1) \tag{19}$$

4. Analysis of Entropy Generation

For the bio-nanofluid system, the irreversibility formulation with R denotes the ideal gas constant and D represents the diffusivity is

$$E'''_{gen}=\frac{\alpha_1}{T_b^2}\left[1+\frac{16T_1^3\sigma^*}{K(T)k^*}\right]\left(\frac{\partial T}{\partial r}\right)^2+\frac{\mu}{T_2}\left(\frac{\partial w}{\partial z}\right)^2+\frac{RD}{C_b}\left(\frac{\partial C}{\partial z}\right)^2+\frac{RD}{T_b}\left(\frac{\partial T}{\partial r}\frac{\partial C}{\partial r}+\frac{\partial C}{\partial z}\frac{\partial T}{\partial z}\right)+\sigma B_o^2 w^2 \tag{20}$$

In Eq. (20), the first term represents the irreversibility due to heat transfer, the second term is entropy generation due to viscous dissipation and third to six terms are irreversibility due to diffusion effect. The seventh term stands for the entropy generation due to magnetic field. The characteristic entropy generation rate is

$$E_0''' = \frac{\alpha_1 \left(T_a - T_b\right)^2}{T_b^2} \tag{21}$$

Notice that irreversibility $N_G(\varsigma)$ in the scaled form is

$$N_G(\varsigma) = \frac{E_{gen}'''}{E_0'''} \tag{22}$$

where E_0''' Dimensional characteristic entropy generation, E_{gen}''' Dimensional entropy generation.

Using Eq. (8), dimensional Eq. (20) converted into the following dimensionless form

$$N_G(\varsigma) = \frac{4}{a^2}\left(1+\frac{4}{3}Rd\right)\theta'^2 + \frac{Br}{\theta_w^2} f'^2 + B_1\left[\left(\frac{\phi_w}{\theta_w}\right)^2 \phi^2 + a^2 \frac{\phi_w}{\theta_w}\phi'\theta' + \frac{\phi_w}{\theta_w}\phi\theta\right] + M\,\mathrm{Pr}\, f'^2 \tag{23}$$

where N_G represents the entropy generation rate, $Br = \frac{4c^2\mu}{\alpha_1(T_w - T_b)}, B_1 = \frac{4RDC_b}{\alpha_1}$, are respectively the Brinkman number, diffusivity constant parameter due to nanoparticle concentration and magnetic field parameter. $\theta_w = \frac{\left(T_a - T_b\right)}{T_b}$, $\phi_w = \frac{\left(C_a - C_b\right)}{C_b}$, are respectively the dimensionless heat and nanoparticle concentration variables.

5. Solution Procedures by HAM

Choosing the initial guesses and the corresponding linear operators as

$$f_o(\zeta) = (1 - e^{-\zeta}), \theta_o = e^{-\zeta}, \phi_o = e^{-\zeta} \tag{24}$$

$$L_f = f''' - f', \quad L_\theta = \theta'' - \theta, \quad L_\phi = \phi'' - \phi \tag{25}$$

satisfying the properties as given below

$$\begin{aligned} L_f\left[C_1 + C_2 e^{\zeta} + C_3 e^{-\zeta}\right] &= 0, \\ L_\theta\left[C_4 e^{\zeta} + C_5 e^{-\zeta}\right] &= 0, \\ L_\phi\left[C_6 e^{\zeta} + C_7 e^{-\zeta}\right] &= 0, \end{aligned} \tag{26}$$

With arbitrary constants $\{C_i\}_{i=1}^{7}$.

To compute the zeroth order form of the problems. Take as follows

$$(1-p)L_f\left[f(\zeta,p)-f_o(\zeta)\right]=p\hbar_f N_f\left[f(\zeta,p),\theta(\zeta,p),\phi(\zeta,p)\right]$$
$$(1-p)L_\theta\left[\theta(\zeta,p)-\theta_o(\zeta)\right]=p\hbar_\theta N_\theta\left[f(\zeta,p),\theta(\zeta,p),\phi(\zeta,p)\right] \quad (27)$$
$$(1-p)L_\phi\left[\phi(\zeta,p)-\phi_o(\zeta)\right]=p\hbar_\phi N_\phi\left[f(\zeta,p),\theta(\zeta,p),\phi(\zeta,p)\right]$$

$$f(1,p)=1,\ f'(\beta_1,p)=0,\ f'(1,p)=1,\theta(1,p)=1,\theta(\beta_1,p)=0,\phi(1,p)=1,\phi(\beta_1,p)=0, \quad (28)$$

with p as the embedding parameter and $\hbar_f,\hbar_\theta,\hbar_\phi$ the non-zero auxiliary parameters. Taking N_f,N_θ,N_ϕ to represent the nonlinear operators and can be obtained through Eq. (10)-(13) as follows

$$N_f\left[f(\zeta,p),\theta(\zeta,p),\phi(\zeta,p)\right]=\frac{2}{\mathrm{Re}}\left(\frac{\partial^2 f(\zeta,p)}{\partial\zeta^2}+\zeta\frac{\partial^3 f(\zeta,p)}{\partial\zeta^3}\right)-M\frac{\partial f(\zeta,p)}{\partial\zeta}$$
$$+f(\zeta,p)\frac{\partial^2 f(\zeta,p)}{\partial\zeta^2}-\left(\frac{\partial f(\zeta,p)}{\partial\zeta}\right)^2+\lambda_1\left(\begin{array}{l}4f(\zeta,p)\frac{\partial f(\zeta,p)}{\partial\zeta}\frac{\partial^3 f(\zeta,p)}{\partial\zeta^3}+\frac{1}{\zeta}f^2(\zeta,p)\frac{\partial^2 f(\zeta,p)}{\partial\zeta^2}\\ -f^2(\zeta,p)\frac{\partial^3 f(\zeta,p)}{\partial\zeta^3}-Mf(\zeta,p)\frac{\partial^2 f(\zeta,p)}{\partial\zeta^2}\end{array}\right) \quad (29)$$
$$-Gr\theta(\zeta,p)+Gm\phi(\zeta,p)$$

$$N_\theta\left[f(\zeta,p),\theta(\zeta,p),\phi(\zeta,p)\right]=(2+Rd)\left(\frac{\partial\theta(\zeta,p)}{\partial\zeta}+\zeta\frac{\partial^2\theta(\zeta,p)}{\partial\zeta^2}\right)$$
$$-Nb\frac{\partial\phi(\zeta,p)}{\partial\zeta}\frac{\partial\theta(\zeta,p)}{\partial\zeta}-Nt\left(\frac{\partial\theta(\zeta,p)}{\partial\zeta}\right)^2+\mathrm{Pr}\left(f(\zeta,p)\frac{\partial\theta(\zeta,p)}{\partial\zeta}-2\theta(\zeta,p)\frac{\partial f(\zeta,p)}{\partial\zeta}\right) \quad (30)$$

$$N_\phi\left[f(\zeta,p),\theta(\zeta,p),\phi(\zeta,p)\right]=Sc\left(\frac{\partial\phi(\zeta,p)}{\partial\zeta}+\zeta\frac{\partial^2\phi(\zeta,p)}{\partial\zeta^2}\right)+f(\zeta,p)\frac{\partial\phi(\zeta,p)}{\partial\zeta}$$
$$-2\phi(\zeta,p)\frac{\partial f(\zeta,p)}{\partial\zeta}+Sc_b\left(\frac{\partial\theta(\zeta,p)}{\partial\zeta}+\zeta\frac{\partial^2\theta(\zeta,p)}{\partial\zeta^2}\right)-\gamma_1\left(\gamma_2-\theta_w\theta(\zeta,p)\right)^n epx\left[\frac{-E}{\left(\gamma_2-\theta_w\theta(\zeta,p)\right)}\right] \quad (31)$$

Taking $p=0$ and $p=1$, the following results are obtained

$$f(\zeta,0)=f_0(\zeta),\theta(\zeta,0)=\theta_0(\zeta),\phi(\zeta,0)=\phi_0(\zeta)$$
$$f(\zeta,1)=f(\zeta),\theta(\zeta,1)=\theta(\zeta),\phi(\zeta,1)=\phi(\zeta) \quad (32)$$

Obviously, when p is increased from 0 to 1, then $f(\zeta,p),\theta(\zeta,p),\phi(\zeta,p)$ vary from $f_o(\zeta),\theta_o(\zeta),\phi_o(\zeta)$ to $f(\zeta),\theta(\zeta),\phi(\zeta)$. Through Taylor's series expansion, the following can be obtained

$$f(\zeta,p)=f_o(\zeta)+\sum_{m=1}^{\infty}f_m(\zeta)p^m,\ f_m(\zeta)=\frac{1}{m!}\frac{\partial^m f(\zeta,p)}{\partial\zeta^m}|_{p=0}$$
$$\theta(\zeta,p)=\theta_o(\zeta)+\sum_{m=1}^{\infty}\theta_m(\zeta)p^m,\theta_m(\zeta)=\frac{1}{m!}\frac{\partial^m\theta(\zeta,p)}{\partial\zeta^m}|_{p=0} \quad (33)$$
$$\phi(\zeta,p)=\phi_o(\zeta)+\sum_{m=1}^{\infty}\phi_m(\zeta)p^m,\phi_m(\zeta)=\frac{1}{m!}\frac{\partial^m\phi(\zeta,p)}{\partial\zeta^m}|_{p=0}$$

The convergence of the series in Eq. (33) depends strongly upon $\hbar_f,\hbar_\theta,\hbar_\phi$. By considering that $\hbar_f,\hbar_\theta,\hbar_\phi$ are selected properly so that the series in Eq. (33) converge at $p=1$, then the following simplifications are achieved

$$f(\zeta)=f_o(\zeta)+\sum_{m=1}^{\infty}f_m(\zeta)$$
$$\theta(\zeta)=\theta_o(\zeta)+\sum_{m=1}^{\infty}\theta_m(\zeta) \quad (34)$$
$$\phi(\zeta)=\phi_o(\zeta)+\sum_{m=1}^{\infty}\phi_m(\zeta)$$

The order m deformation of the problem can be constructed as follow

$$L_f\left[f_m(\zeta)-\eta_m f_{m-1}(\zeta)\right]=\hbar_f R_f^m(\zeta)$$
$$L_\theta\left[\theta_m(\zeta)-\eta_m\theta_{m-1}(\zeta)\right]=\hbar_\theta R_\theta^m(\zeta) \quad (35)$$
$$L_\phi\left[\phi_m(\zeta)-\eta_m\phi_{m-1}(\zeta)\right]=\hbar_\phi R_\phi^m(\zeta)$$

$$f_m(1)=f'(1)=f'(\beta_1)=0,\theta_m(1)=\theta_m(\beta_1)=0,\phi_m(1)=\phi_m(\beta_1)=0 \quad (36)$$

where $R_f^m(\zeta),R_\theta^m(\zeta),R_\phi^m(\zeta)$ and can be obtained as

$$R_f^m(\zeta)=\tfrac{2}{\mathrm{Re}}\left(f''_{m-1}(\zeta)+\zeta f'''_{m-1}(\zeta)\right)-Mf'_{m-1}+\sum_{k=0}^{m-1}f_{m-1-k}f''_k(\zeta)-\sum_{k=0}^{m-1}f'_{m-1-k}f'_k(\zeta)$$
$$+\lambda_1\begin{pmatrix}4\sum_{k=0}^{m-1}\left(\sum_{r=0}^{k}f_{m-1-k}f'_{k-r}(\zeta)\right)f''_r(\zeta)+\frac{1}{\zeta}\sum_{k=0}^{m-1}\left(\sum_{r=0}^{k}f_{m-1-k}f_{k-r}(\zeta)\right)f'''_r(\zeta)\\-2\sum_{k=0}^{m-1}\left(\sum_{r=0}^{k}f_{m-1-k}f_{k-r}(\zeta)\right)f'''_r(\zeta)-2M\sum_{k=0}^{m-1}f_{m-1-k}f''_k(\zeta)\end{pmatrix}-Gr\theta_m(\zeta)+Gm\phi_m(\zeta) \quad (37)$$

$$R_\theta^m(\zeta)=(2+Rd)\left(\theta'_{m-1}(\zeta)+\zeta\theta''_{m-1}(\zeta)\right)-Nb\sum_{k=0}^{m-1}\phi'_{m-1-k}\theta'_k-Nt\sum_{k=0}^{m-1}\theta'_{m-1-k}\theta'_k+\mathrm{Pr}\left(\sum_{k=0}^{m-1}f_{m-1-k}\theta'_k-2\sum_{k=0}^{m-1}\phi'_{m-1-k}\theta_k\right) \quad (38)$$

$$R_{\phi}^{m}(\zeta)=Sc\left(\phi_{m-1}^{'}(\zeta)+\zeta\phi_{m-1}^{''}(\zeta)\right)+\sum_{k=0}^{m-1}\phi_{m-1-k}^{'}(\zeta)\,f_{k}(\zeta)-2\sum_{k=0}^{m-1}f_{m-1-k}^{'}(\zeta)\phi_{k}(\zeta)$$
$$+Sc_{b}\left(\theta_{m-1}^{'}(\zeta)+\zeta\theta_{m-1}^{''}(\zeta)\right)-\gamma_{1}\left(\gamma_{2}-\theta_{w}\theta_{m}(\zeta)\right)^{n}epx\left[\frac{-E}{\left(\gamma_{2}-\theta_{w}\theta_{m}(\zeta)\right)}\right] \tag{39}$$

$$\eta_{m}=\begin{Bmatrix}0, & m\le 1\\ 1, & m>1\end{Bmatrix} \tag{40}$$

The general solutions are given by

$$\begin{aligned}f_{m}(\zeta)&=f_{m}^{*}(\zeta)+C_{1}+C_{2}e^{\zeta}+C_{3}e^{-\zeta}\\ \theta_{m}(\zeta)&=\theta_{m}^{*}(\zeta)+C_{4}e^{\zeta}+C_{5}e^{-\zeta}\\ \phi_{m}(\zeta)&=\phi_{m}^{*}(\zeta)+C_{6}e^{\zeta}+C_{7}e^{-\zeta}\end{aligned} \tag{41}$$

with $f_{m}^{*}(\zeta),\theta_{m}^{*}(\zeta),\phi_{m}^{*}(\zeta)$ are the special solutions.

6. Results and Discussion

The graphs are prepared using the following set of parameters $\lambda_{1}=Gr=Gm=0.3$, $\beta=\gamma_{1}=\gamma_{2}=\mathrm{Re}=Rd=Sc=E=M=0.4$, $Nb=Nt=0.5$, and $\beta_{1}=2$. To achieve acceptable results, Liao [44-46] introduced h curves for the convergence of the series solution. Therefore, the acceptable h-curves for $f(\zeta)$, $\theta(\zeta)$ and $\phi(\zeta)$ are drawn in the ranges $-4\le h\le 4$, $-2\le h\le 2$, and $-4\le h\le 4$ in Figure 2, Figure 3 and Figure 4 respectively.

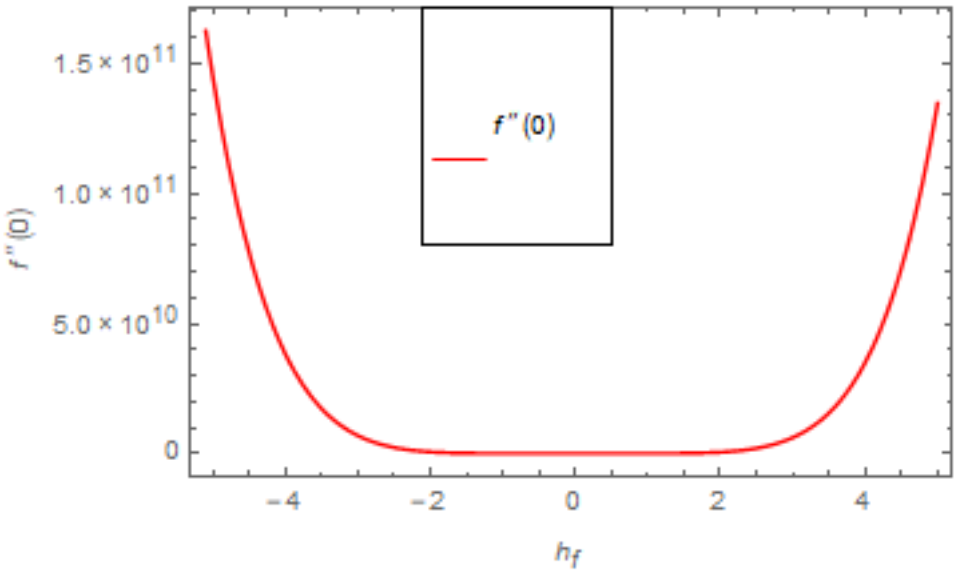

Fig. 2. $h-curve$ of $f'(\zeta)$

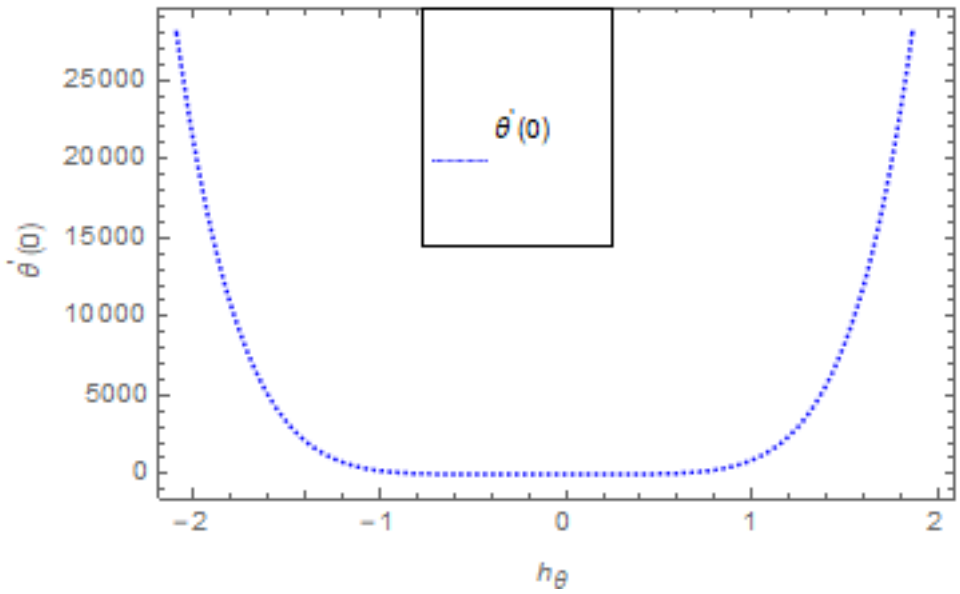

Fig. 3. $h-curve$ of $\theta(\zeta)$

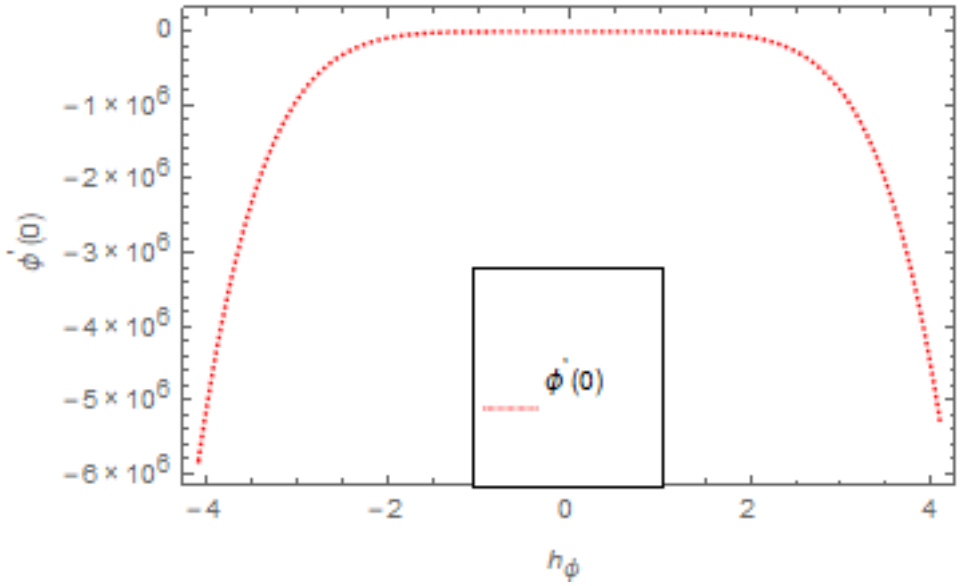

Fig. 4. $h-curve$ of $\phi(\zeta)$

The viscoelastic nano-liquid dynamic with coolant and shielding paint or film are sprayed on a stretching cylinder. Figure 5 depicts the normalized spray rate m_2, which is functionally correlated with film size. The film size naturally increases with the spray rate at simultaneously in a nonlinear fashion. The film's outer surface as observed may be harmed if the spray is not uniform. Spraying also improves cooling because it creates a thinner boundary layer.

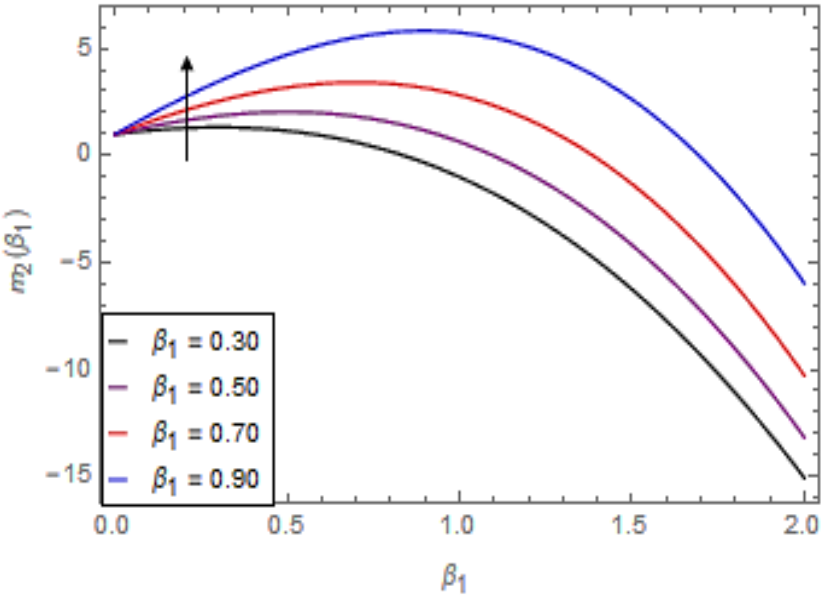

Fig. 5. Effect of β_1 on $m_2(\beta_1)$

Figure 6 shows that the velocity is a decreasing function of the magnetic field parameter M. In general, when a magnetic field is applied to a conduction-capable fluid flow, the momentum boundary layer becomes thin. The possible explanation for this is that throughout this process, resistance forces known as Lorentz forces are generated, which have a negative impact on fluid flow. This force slows the velocity of the nanofluid as it passes through the vertical surface.

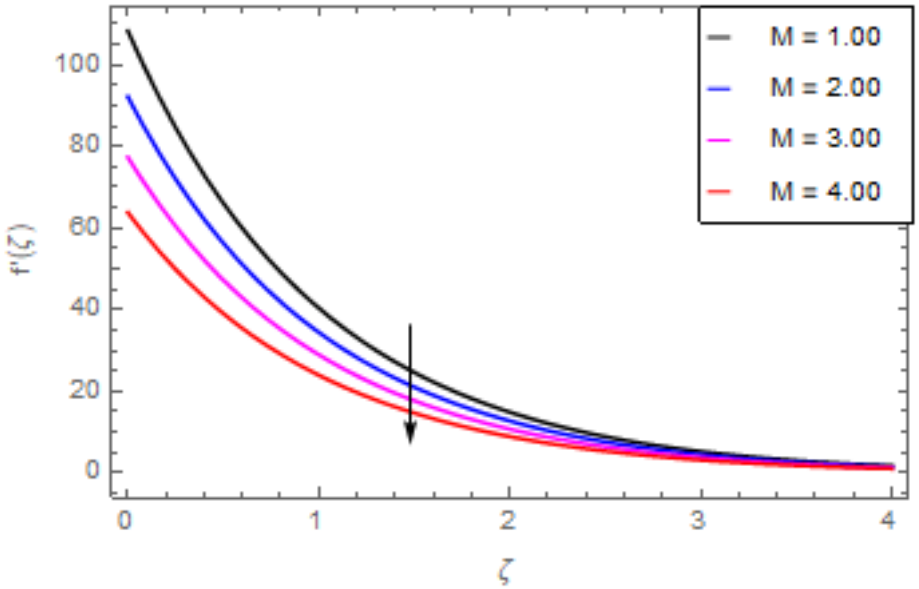

Fig. 6. Effect of M on $f'(\zeta)$

Figure 7 depicts that by increasing the viscoelastic parameter the velocity decreases and hence momentum boundary layer thickness weakens. Figure 8 illustrates that the velocity increases with the Grashof number as a consequence of the buoyancy force's dominant effects in the core part, which causes changes in velocity and high viscous effects across the walls.

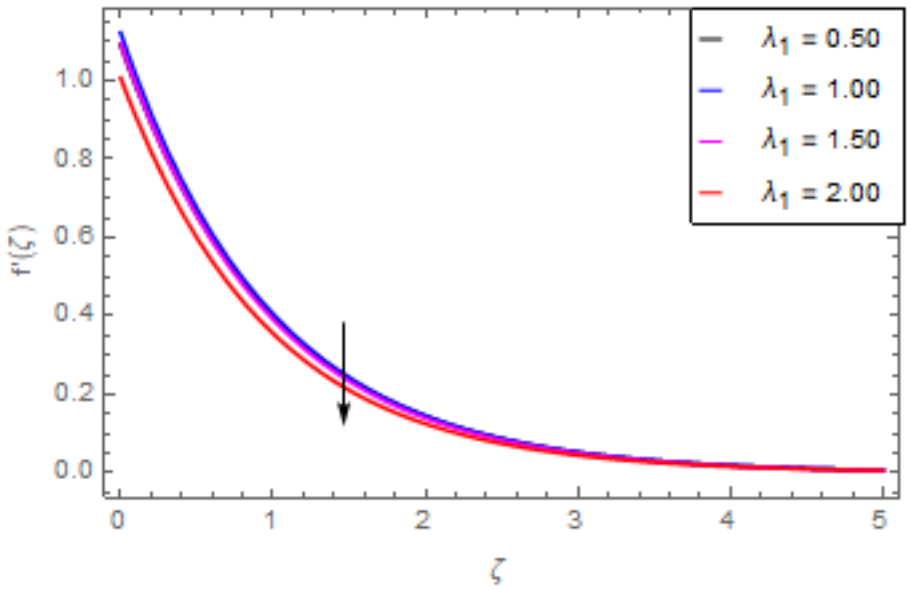

Fig. 7. Effect of λ_1 on $f'(\zeta)$

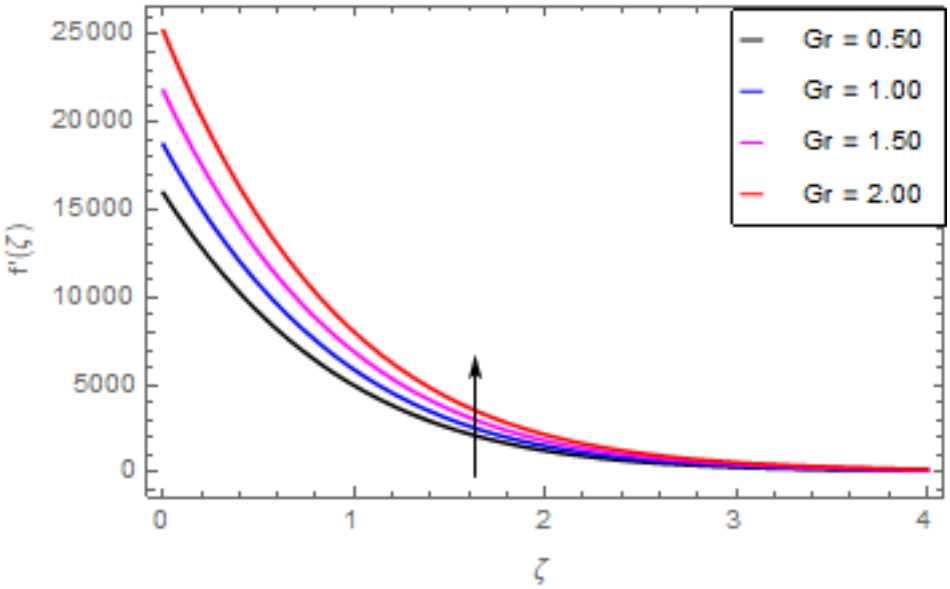

Fig. 8. Effect of Gr on $f'(\zeta)$

As shown in Figure 9, the velocity increased as the Reynolds number increased. This is due to the fact that as the Reynolds number increases, the inertial force dominates the flow more than the viscous forces. High viscous forces are highly resistive to fluid flow, and strong inertial forces reduce the flow of the boundary layer. When Re is small, then it means there exists small inertial effect compared to that of viscous effect. Since $\mathrm{Re} = \frac{ca^2}{\nu_f}$ so for Re = 0, the stretching rate c tends to vanishing since the cylinder radius a cannot be zero in the present case. Also, the thickness is made infinite for finite deposition rate and the steady form cannot exist.

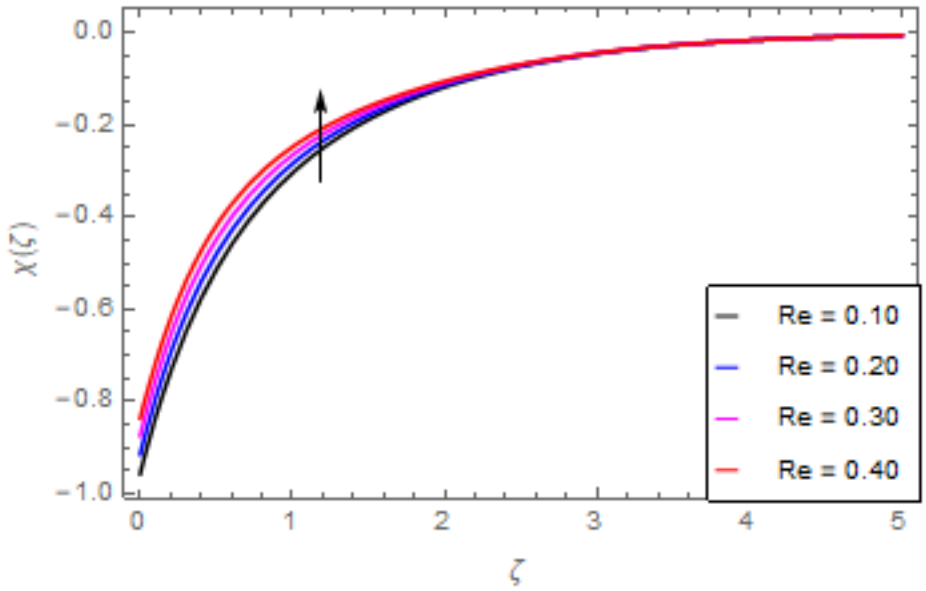

Fig. 9. Effect of Re on $f'(\zeta)$

Figure 10 shows that increasing the magnetic field parameter values raises the temperature of the nanofluid. The magnetic field parameter generates a resistive force that works in the opposite direction of the flow field and increases the thickness of the thermal boundary layer.

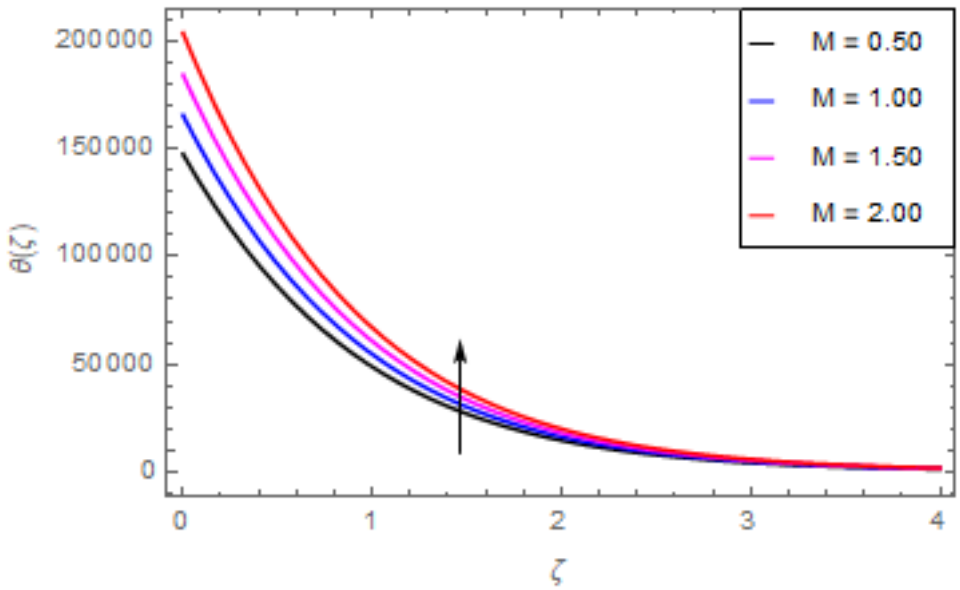

Fig. 10. Effect of M on $\theta(\zeta)$

Figure 11 shows that as the Prandtl number increases, the temperature of the nanofluid decreases, and thus the thermal boundary layer decreases, indicating that effective cooling of the nanofluid occurs quickly. Given the small size of the motion layer, the impact of a high Prandtl number is even more obvious.

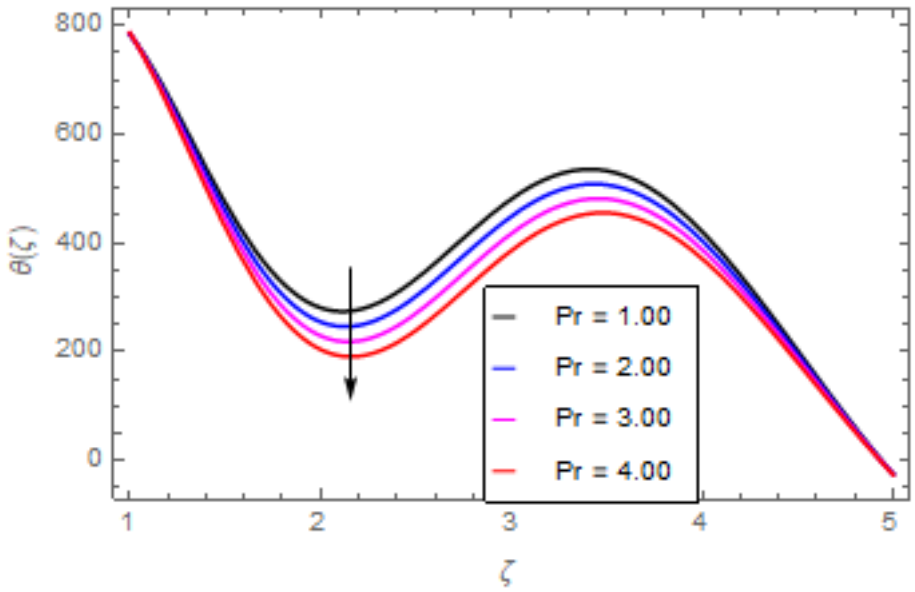

Fig. 11. Effect of Pr on $\theta(\zeta)$

Figure 12 shows that increasing the Brownian motion parameter causes an increase in fluid temperature, resulting in a decrease in friction on the free surface of nanoparticles, this demonstrates that the thickness of the thermal boundary layer increases, indicating that nanoparticles play an important role in improving convection.

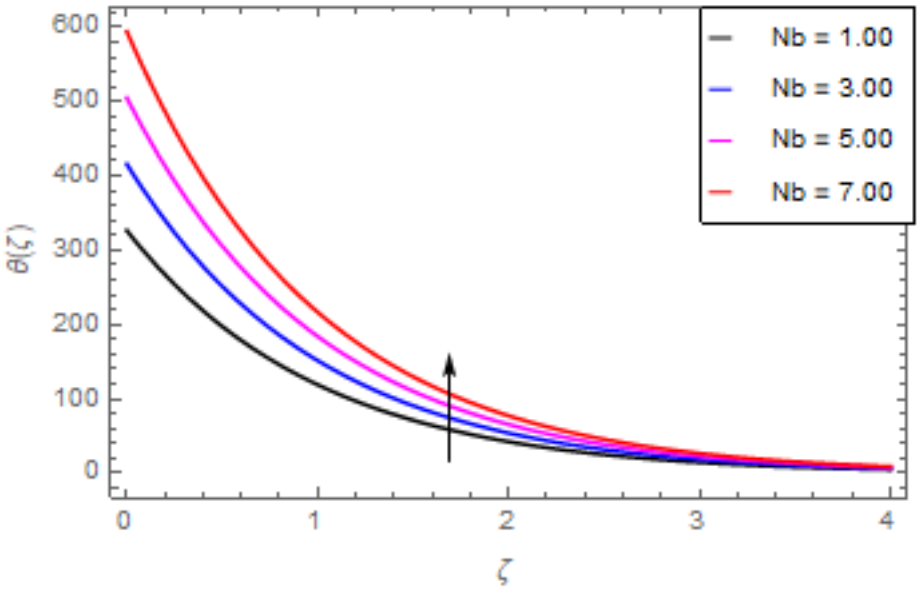

Fig. 12. Effect of Nb on $\theta(\zeta)$

Figure 13 shows that as the Thermophoresis parameter values increase, the temperature of the nanofluid decreases. Thermophoresis is the phenomenon of particle diffusion caused by a temperature gradient effect. The force that transfers nanoparticles to the surrounding fluid as a result of a temperature gradient is known as thermophoretic force. Increased thermophoretic force results in more nanoparticles being transferred to the fluid layer.

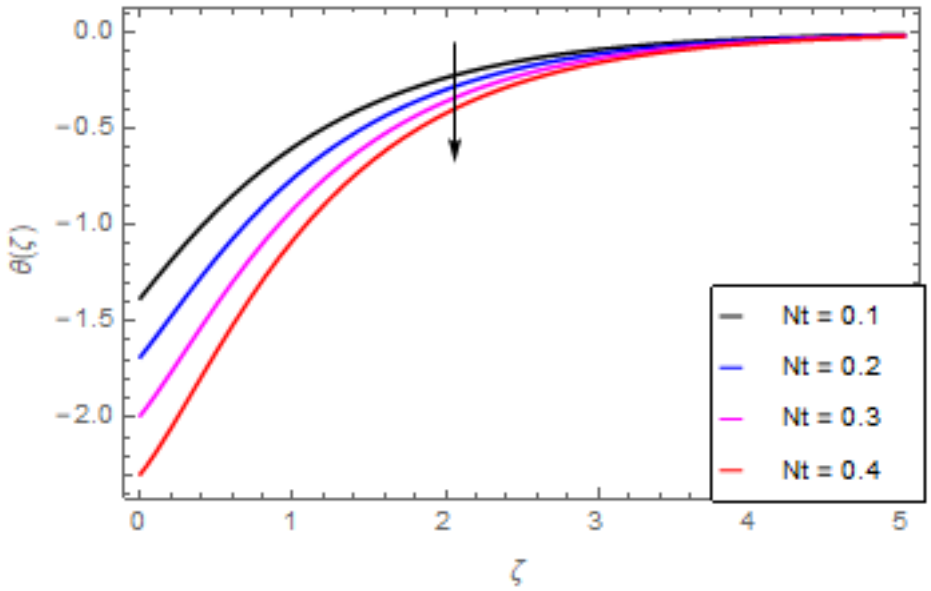

Fig. 13. Effect of Nt on $\theta(\zeta)$

As shown in Figure 14, the radiation parameter is used to add heat to the temperature of the nanoparticles as the temperature of the nanofluid rises. Thermal radiation analysis is essential in the cooling of the cylinder and present study incorporate with the many published results. The temperature distribution is influenced by the thin film parameter. The thermal boundary surface's temperature is high and small, as is the transverse distance. For larger quantities, the film thickness parameter slows down the temperature, as shown in Figure 15. The heat transfer is improved by thinning the nanofluid. In the current situation, however, it is depreciating. The possible explanation for this is that as the thickness of the fluid film increases, so does the mass of the fluid, which exhausts the temperature. Mostly as consequence, heat enters the fluid and the environment cools.

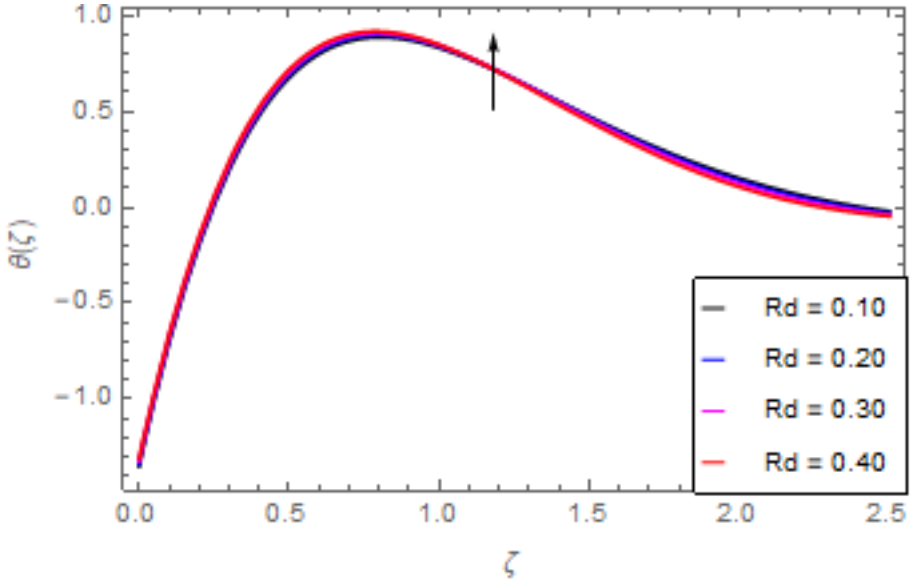

Fig. 14. Effect of Rd on $\theta(\zeta)$

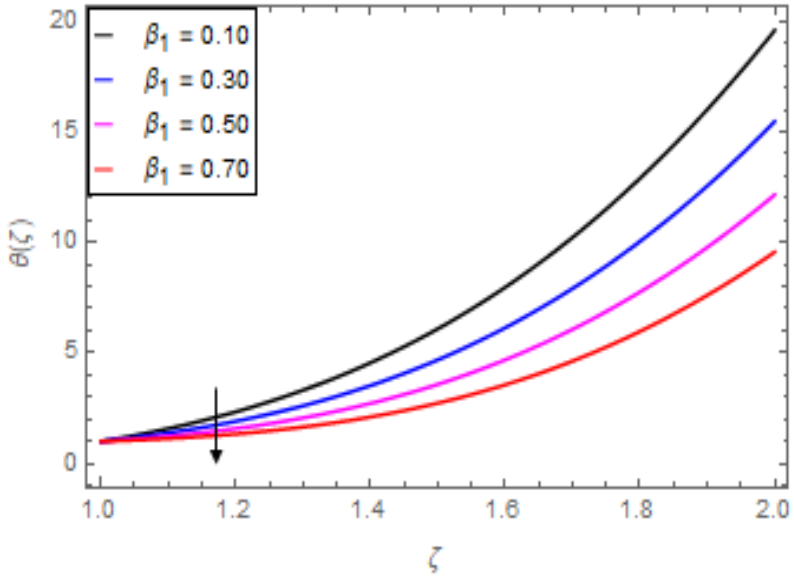

Fig. 15. Effect of β_1 on $\theta(\zeta)$

Figure 16 and Figure 17 depict the effect of the activation energy parameter and the binary chemical reaction parameter on the concentration profile, demonstrating that it is increased with larger activation energy parameter values and decelerated with larger chemical reaction parameter values, respectively. The Schmidt number is related to mass diffusions and thus increases mass diffusivity values, resulting in a decrease in nanoparticle concentration due to less mass diffusion transportation, as shown in Figure 18.

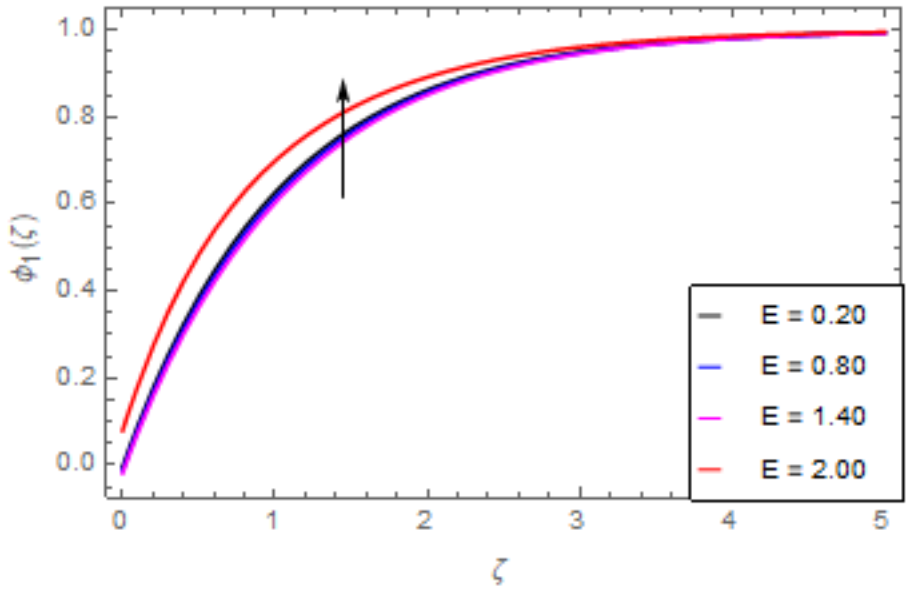

Fig. 16. Effect of E on $\phi(\zeta)$

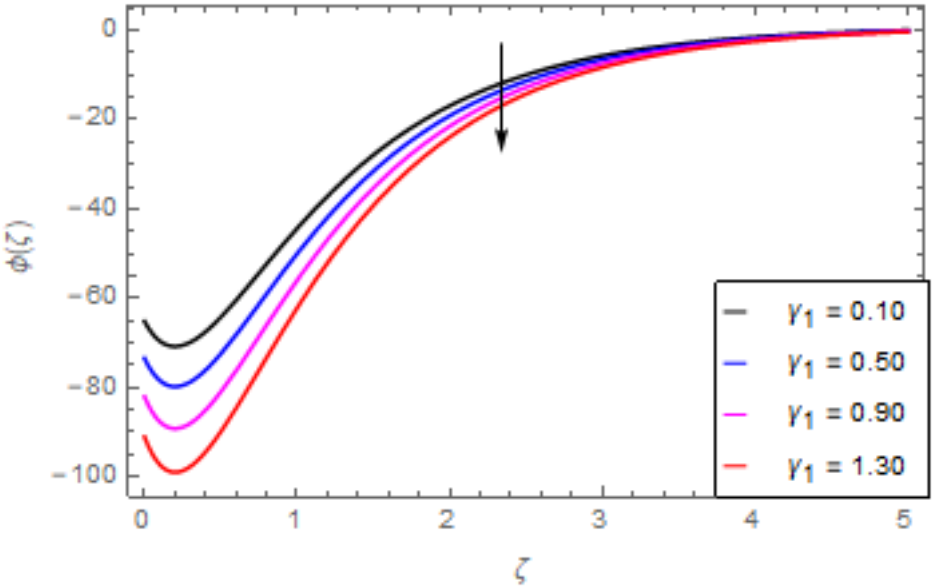

Fig. 17. Effect of γ_1 on $\phi(\zeta)$

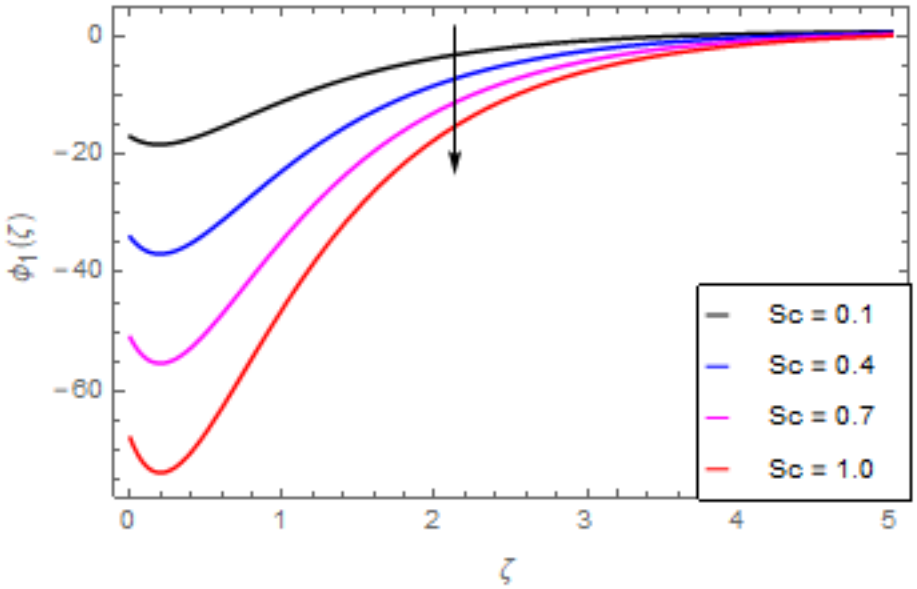

Fig. 18. Effect of Sc on $\phi(\zeta)$

Increasing the magnetic field parameter causes a slight increase in entropy generation in general. Because the magnetic field parameter has little effect on entropy generation, a large change in the magnetic field parameter results in a small change in entropy, as illustrated in Figure 19.

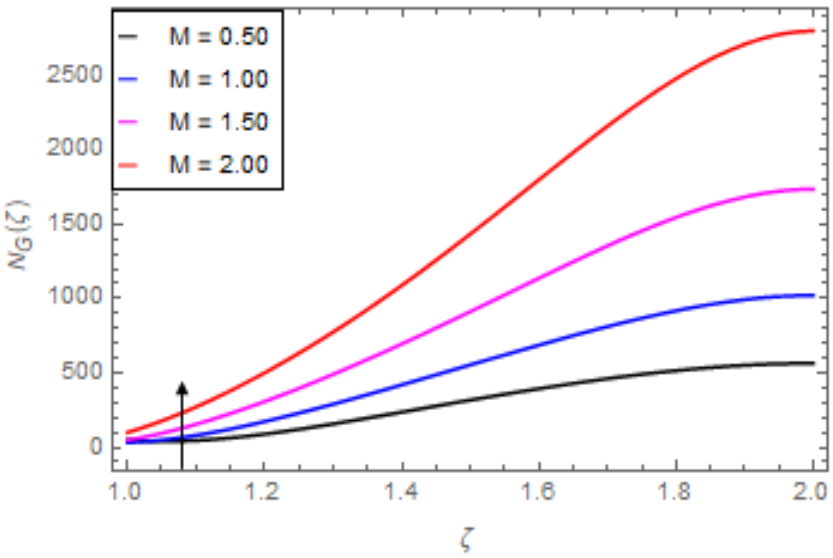

Fig. 19. Effect of M on $N_G(\zeta)$

Figure 20 shows that as the Brinkmann number increases, so does the generation of entropy. Physically, this is of real significance since $Br(=\ \mathrm{Pr}\ Ec)$ is an irreversibility coefficient of fluid friction. The Prandtl number is defined as the ratio of thermal to momentum diffusivity, whereas the Eckert number is defined as the conversion of kinetic energy into heat in the flow domain via viscous dissipation. The generation of entropy increases as viscous dissipation increases.

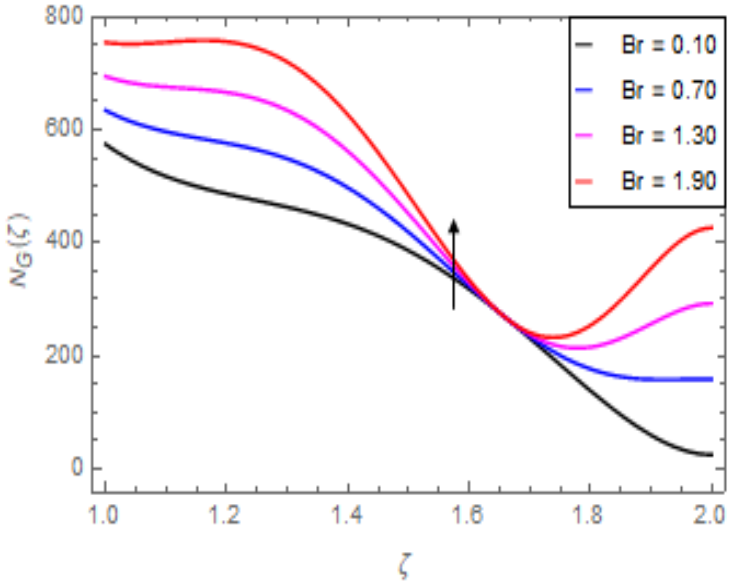

Fig. 20. Effect of Br on $N_G(\zeta)$

Figure 21 depicts how the rate of entropy generation in the flow increases as the thermal radiation parameter increases. This is because the emission through the thermal radiation parameter has increased.

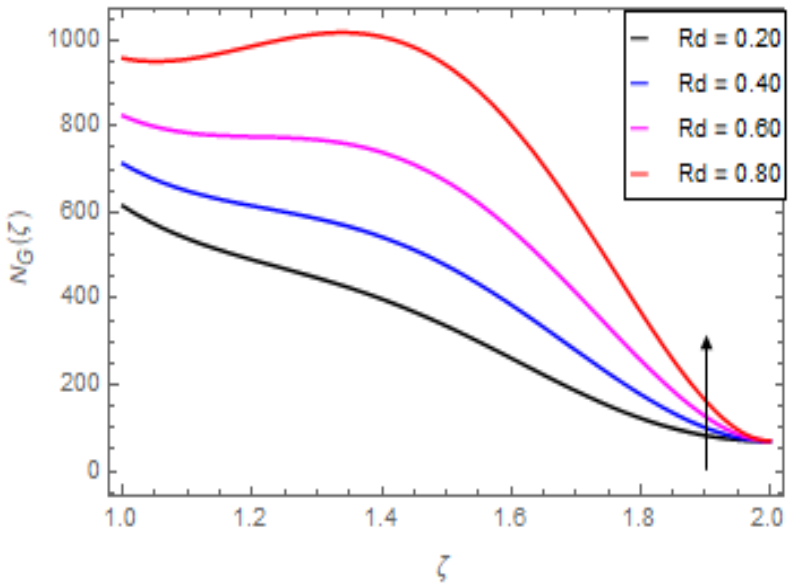

Fig. 21. Effect of Rd on $N_G(\zeta)$

6.1 Table Discussion

The current work is compared to the published work by Hayat *et al.,* [39] for various Prandtl number $\Pr$ values, and the results show good resemblance, as seen in Table 1.

Table 1
Comparison of $-\theta'(1)$ for various values of $\Pr$ the present research with published paper

$\Pr$	Hayat *et al.,* [39]	Present work
1.0	-1.0000	-1.0000
	0.0	0.0
	0.5832	0.5832
	1.0000	1.0000
	1.3332	1.3334
10	-10.0000	-10.0000
	0.0	0.0
	2.3080	2.3076
	3.7207	3.7210
	4.7969	4.7971
0.9	1.2507	1.2507
0.8	1.1662	1.1659
0.7	1.0791	1.0793

Table 2 shows the convergence of series solutions for different order of approximation.

Table 2
Convergence of series solutions for different order of approximations

Oder of Approximation	$-f''(1)$	$-\theta'(1)$	$-\phi'(1)$
1	0.7331	0.6513	0.6033
10	0.6282	0.6239	0.6000
20	0.5121	0.6070	0.5891
21	0.5001	0.5969	0.5891
25	0.4990	0.5969	0.5891
30	0.4990	0.5969	0.5891

Table 3, Table 4 and Table 5 showed the numerical values of the physical quantities accessing the effect of different parameters.

Table 3
Variation in skin friction coefficient $-f''(1)$ for M, λ_1, Re, Gr and Gm

M	λ_1	Re	Gr	Gm	$-f''(1)$
0.4	0.3	0.4	0.3	0.3	0.4231
0.6					0.3231
0.8					0.2231
1.0					0.1231
	0.4				0.1231
	0.5				0.0231
	0.6				0.1031
		0.7			0.1031
		1.0			0.1231
		1.3			0.0231
			0.5		0.0231
			0.7		0.1230
			0.9		0.1201
				0.5	0.1031
				0.7	0.0031
				0.9	0.1031

Table 4
Variation in Nusselt number $-\theta'(1)$ for M, λ_1, Pr, Nb, Nt and Rd

M	λ_1	Pr	Nb	Nt	Rd	$-\theta'(1)$
0.4	0.3	0.7	0.3	0.3	0.4	0.2764
0.2						0.2763
0.6						0.2755
1.0						0.2745
	0.4					0.2735
	0.5					0.2725
	0.6					0.2715
		1.0				0.2754
		1.3				0.2753
		1.6				0.2760
			1.0			0.2761
			1.7			0.2762
			2.4			0.2736
				1.0		0.2735
				1.7		0.2734
				2.4		0.2733
					1.0	0.2732
					1.6	0.2731
					2.0	0.2730

Table 5
Variation in Sherwood number $-\phi'(1)$ for λ_1, Pr, Nb, Nt and E

λ_1	Nb	Nt	γ_1	E	$-\phi'(1)$
0.3	0.3	0.3	0.4	0.4	0.15479
0.5					0.15478
0.7					0.15477
0.9					0.15476
	1.0				0.15475
	1.7				0.15474
	2.4				0.15473
		0.6			0.15472
		0.9			0.15471
		1.2			0.15470
			0.9		0.15469
			1.4		0.15468
			1.9		0.15467
				0.8	0.15468
				1.3	0.15467
				1.8	0.15466

7. Conclusions

The mass and heat transfer flow of the viscoelastic nanoliquid film sprayed on the stretching cylinder taking to account the effect of activation energy and entropy measure is evaluated. The solution of the problem obtained using HAM and presented the result using graphs. These results shows that an effective flow and cooling process of heat exchange of innovative scientific and engineering are observed. The most important findings are

i. The velocity decreases as the magnetic field and viscoelastic parameters are increased.
ii. The temperature increases with the increase in Brownian motion parameter and decreases with the Thermophoresis parameter and Prandtl number.
iii. The activation energy parameter causes the nanoparticle concentration to rise, while the thermal radiation and chemical reaction parameters, as well as the Schmidt number, cause it to decline.
iv. The generation of entropy increases with the increase of all parameters such as magnetic field and thermal radiation parameters and Brinkman number.
v. The spray rate increase in a nonlinear fashion with the thickness of the film.

Acknowledgments
The authors appreciate the financial support allotted by King Mongkut's University of Technology Thonburi through the "KMUTT 55th Anniversary Commemorative Fund". The first author is supported by the Petchra Pra Jom Klao Doctoral Scholarship Academic for PhD studies at KMUTT. This research was accomplished with the help of the Theoretical and Computational Science (TaCS-CoE) Center, Faculty of Science, KMUTT. We are obliged to the respectable referees for their important and fruitful comments to enhance the quality of this article.

References

[1] Albano, P. G., C. A. Borghi, A. Cristofolini, M. Fabbri, Y. Kishimoto, F. Negrini, H. Shibata, and M. Zanetti. "Industrial applications of magnetohydrodynamics at the University of Bologna." *Energy Conversion and Management* 43, no. 3 (2002): 353-363. https://doi.org/10.1016/S0196-8904(01)00102-9

[2] Han, Shihao, Liancun Zheng, Chunrui Li, and Xinxin Zhang. "Coupled flow and heat transfer in viscoelastic fluid with Cattaneo-Christov heat flux model." *Applied Mathematics Letters* 38 (2014): 87-93. https://doi.org/10.1016/j.aml.2014.07.013

[3] Mrokowska, Magdalena M., and Anna Krztoń-Maziopa. "Viscoelastic and shear-thinning effects of aqueous exopolymer solution on disk and sphere settling." *Scientific Reports* 9, no. 1 (2019): 1-13. https://doi.org/10.1038/s41598-019-44233-z

[4] Li, Jing, Liancun Zheng, and Lin Liu. "MHD viscoelastic flow and heat transfer over a vertical stretching sheet with Cattaneo-Christov heat flux effects." *Journal of Molecular Liquids* 221 (2016): 19-25. https://doi.org/10.1016/j.molliq.2016.05.051

[5] Kumar, Anantha, Ramana Reddy JV, V. Sugunamma, and N. Sandeep. "Impact of cross diffusion on MHD viscoelastic fluid flow past a melting surface with exponential heat source." *Multidiscipline Modeling in Materials and Structures* (2018).

[6] Kumar, B. Rushi, and R. Sivaraj. "Heat and mass transfer in MHD viscoelastic fluid flow over a vertical cone and flat plate with variable viscosity." *International Journal of Heat and Mass Transfer* 56, no. 1-2 (2013): 370-379. https://doi.org/10.1016/j.ijheatmasstransfer.2012.09.001

[7] Ganesh, N. Vishnu, Qasem M. Al-Mdallal, and Ali J. Chamkha. "A numerical investigation of Newtonian fluid flow with buoyancy, thermal slip of order two and entropy generation." *Case Studies in Thermal Engineering* 13 (2019): 100376. https://doi.org/10.1016/j.csite.2018.100376

[8] Ganesh, N. Vishnu, Qasem M. Al-Mdallal, Sara Al Fahel, and Shymaa Dadoa. "Riga-Plate flow of γ Al2O3-water/ethylene glycol with effective Prandtl number impacts." *Heliyon* 5, no. 5 (2019): e01651. https://doi.org/10.1016/j.heliyon.2019.e01651

[9] Ganesh, N. Vishnu, Qasem M. Al-Mdallal, and R. Kalaivananc. "Exact solution for heat transport of Newtonian fluid with quadratic order thermal slip in a porous medium." *Advances in the Theory of Nonlinear Analysis and its Application* 5, no. 1 (2021): 39-48. https://doi.org/10.31197/atnaa.749630

[10] Chu, Yu-Ming, Umair Khan, Anum Shafiq, and A. Zaib. "Numerical simulations of time-dependent micro-rotation blood flow induced by a curved moving surface through conduction of gold particles with non-uniform heat sink/source." *Arabian Journal for Science and Engineering* 46, no. 3 (2021): 2413-2427. https://doi.org/10.1007/s13369-020-05106-0

[11] Rashidi, M. M., M. Ali, N. Freidoonimehr, B. Rostami, and M. Anwar Hossain. "Mixed convective heat transfer for MHD viscoelastic fluid flow over a porous wedge with thermal radiation." *Advances in Mechanical Engineering* 6 (2014): 735939. https://doi.org/10.1155/2014/735939

[12] Choi, S. US, and Jeffrey A. Eastman. *Enhancing thermal conductivity of fluids with nanoparticles*. No. ANL/MSD/CP-84938; CONF-951135-29. Argonne National Lab., IL (United States), 1995.

[13] Buongiorno, J. "Convective transport in nanofluids." *Journal of Heat Transfer* 128, no. 3 (2006): 240-250. https://doi.org/10.1115/1.2150834

[14] Chakraborty, Samarshi, and Pradipta Kumar Panigrahi. "Stability of nanofluid: A review." *Applied Thermal Engineering* 174 (2020): 115259. https://doi.org/10.1016/j.applthermaleng.2020.115259

[15] Ellahi, Rahmat, Ahmed Zeeshan, Farooq Hussain, and Tehseen Abbas. "Thermally charged MHD bi-phase flow coatings with non-Newtonian nanofluid and hafnium particles along slippery walls." *Coatings* 9, no. 5 (2019): 300. https://doi.org/10.3390/coatings9050300

[16] Ganesh, N. Vishnu, Qasem M. Al-Mdallal, and P. K. Kameswaran. "Numerical study of MHD effective Prandtl number boundary layer flow of γ Al2O3 nanofluids past a melting surface." *Case Studies in Thermal Engineering* 13 (2019): 100413. https://doi.org/10.1016/j.csite.2019.100413

[17] Ganesh, N. Vishnu, Qasem M. Al-Mdallal, K. Reena, and Sidra Aman. "Blasius and Sakiadis slip flow of H2O-C2H6O2 (50: 50) based nanoliquid with different geometry of boehmite alumina nanoparticles." *Case Studies in Thermal Engineering* 16 (2019): 100546. https://doi.org/10.1016/j.csite.2019.100546

[18] Ganesh, N. Vishnu, P. K. Kameswaran, Qasem M. Al-Mdallal, A. K. Hakeem, and B. Ganga. "Non-Linear thermal radiative marangoni boundary layer flow of gamma Al2O3 nanofluids past a stretching sheet." *Journal of Nanofluids* 7, no. 5 (2018): 944-950. https://doi.org/10.1166/jon.2018.1510

[19] Mebarek-Oudina, Fateh, Ahmed Kadhim Hussein, Obai Younis, Sara Rostami, and Rasoul Nikbakhti. "Natural convection enhancement in the annuli between two homocentric cylinders by using ethylene glycol/water based

titania nanofluid." *Journal of Advanced Research in Fluid Mechanics and Thermal Sciences* 80, no. 2 (2021): 56-73. https://doi.org/10.37934/arfmts.80.2.5673

[20] Zaharudin, Rozaidi, and Radhiyah Abd Aziz. "Thermal Conductivity and Stability Studies of Cooking and Waste Cooking Oil as a Based Fluid of TiO2 Nanofluid for Carbon Steel Quenching Process." *Journal of Advanced Research in Fluid Mechanics and Thermal Sciences* 78, no. 2 (2021): 22-33. https://doi.org/10.37934/arfmts.78.2.2233

[21] Faizal, Nur Faizzati Ahmad, Norihan Md Ariffin, Yong Faezah Rahim, Mohd Ezad Hafidz Hafidzuddin, and Nadihah Wahi. "MHD and Slip Effect in Micropolar Hybrid Nanofluid and Heat Transfer over a Stretching Sheet with Thermal Radiation and Non-uniform Heat Source/Sink." *CFD Letters* 12, no. 11 (2020): 121-130. https://doi.org/10.37934/cfdl.12.11.121130

[22] Ganesh, N. Vishnu, Ali J. Chamkha, Qasem M. Al-Mdallal, and P. K. Kameswaran. "Magneto-Marangoni nano-boundary layer flow of water and ethylene glycol based γ Al2O3 nanofluids with non-linear thermal radiation effects." *Case Studies in Thermal Engineering* 12 (2018): 340-348. https://doi.org/10.1016/j.csite.2018.04.019

[23] Ganesh, N. Vishnu, Shumaila Javed, Qasem M. Al-Mdallal, R. Kalaivanan, and Ali J. Chamkha. "Numerical study of heat generating γ Al2O3-H2O nanofluid inside a square cavity with multiple obstacles of different shapes." *Heliyon* 6, no. 12 (2020): e05752. https://doi.org/10.1016/j.heliyon.2020.e05752

[24] Khan, Umair, Iskandar Waini, Anuar Ishak, and Ioan Pop. "Unsteady hybrid nanofluid flow over a radially permeable shrinking/stretching surface." *Journal of Molecular Liquids* 331 (2021): 115752. https://doi.org/10.1016/j.molliq.2021.115752

[25] Khan, Umair, Sardar Bilal, A. Zaib, O. D. Makinde, and Abderrahim Wakif. "Numerical simulation of a nonlinear coupled differential system describing a convective flow of Casson gold-blood nanofluid through a stretched rotating rigid disk in the presence of Lorentz forces and nonlinear thermal radiation." *Numerical Methods for Partial Differential Equations* (2020). https://doi.org/10.1002/num.22620

[26] Ellahi, Rahmat, Ahmed Zeeshan, Farooq Hussain, and Tehseen Abbas. "Study of shiny film coating on multi-fluid flows of a rotating disk suspended with nano-sized silver and gold particles: A comparative analysis." *Coatings* 8, no. 12 (2018): 422. https://doi.org/10.3390/coatings8120422

[27] Khan, Noor Saeed, Taza Gul, Saeed Islam, Ilyas Khan, Aisha M. Alqahtani, and Ali Saleh Alshomrani. "Magnetohydrodynamic nanoliquid thin film sprayed on a stretching cylinder with heat transfer." *Applied Sciences* 7, no. 3 (2017): 271. https://doi.org/10.3390/app7030271

[28] Palwasha, Zaman, Saeed Islam, Noor Saeed Khan, and Hamza Ayaz. "Non-Newtonian nanoliquids thin-film flow through a porous medium with magnetotactic microorganisms." *Applied Nanoscience* 8, no. 6 (2018): 1523-1544. https://doi.org/10.1007/s13204-018-0834-5

[29] Hartig, Klaus, and Annette J. Krisko. "Thin film coating having transparent base layer." *U.S. Patent 6,919,133*, issued July 19, 2005.

[30] Arrhenius, Svante. "Über die Dissociationswärme und den Einfluss der Temperatur auf den Dissociationsgrad der Elektrolyte." *Zeitschrift für physikalische Chemie* 4, no. 1 (1889): 96-116. https://doi.org/10.1515/zpch-1889-0408

[31] Bestman, A. R. "Natural convection boundary layer with suction and mass transfer in a porous medium." *International Journal of Energy Research* 14, no. 4 (1990): 389-396. https://doi.org/10.1002/er.4440140403

[32] Ramesh, G. K. "Analysis of active and passive control of nanoparticles in viscoelastic nanomaterial inspired by activation energy and chemical reaction." *Physica A: Statistical Mechanics and its Applications* 550 (2020): 123964. https://doi.org/10.1016/j.physa.2019.123964

[33] Kalaivanan, R., N. Vishnu Ganesh, and Qasem M. Al-Mdallal. "An investigation on Arrhenius activation energy of second grade nanofluid flow with active and passive control of nanomaterials." *Case Studies in Thermal Engineering* 22 (2020): 100774. https://doi.org/10.1016/j.csite.2020.100774

[34] Kalaivanan, R., N. Vishnu Ganesh, and Qasem M. Al-Mdallal. "Buoyancy driven Flow of a Second-Grade Nanofluid flow Taking into Account the Arrhenius Activation Energy and Elastic Deformation: Models and Numerical Results." *Fluid Dynamics & Materials Processing* 17, no. 2 (2021): 319-332. https://doi.org/10.32604/fdmp.2021.012789

[35] Tahir, Hassan, Umair Khan, Anwarud Din, Yu-Ming Chu, and Noor Muhammad. "Heat transfer in a ferromagnetic chemically reactive species." *Journal of Thermophysics and Heat Transfer* 35, no. 2 (2021): 402-410. https://doi.org/10.2514/1.T6143

[36] Abdelmalek, Zahra, B. Mahanthesh, Md Faisal Md Basir, Maria Imtiaz, Joby Mackolil, Noor Saeed Khan, Hossam A. Nabwey, and I. Tlili. "Mixed radiated magneto Casson fluid flow with Arrhenius activation energy and Newtonian heating effects: Flow and sensitivity analysis." *Alexandria Engineering Journal* 59, no. 5 (2020): 3991-4011. https://doi.org/10.1016/j.aej.2020.07.006

[37] Wang, Ch Y. "Fluid flow due to a stretching cylinder." *The Physics of Fluids* 31, no. 3 (1988): 466-468. https://doi.org/10.1063/1.866827

[38] Bachok, Norfifah, and Anuar Ishak. "Flow and heat transfer over a stretching cylinder with prescribed surface heat flux." *Malaysian Journal of Mathematical Sciences* 4, no. 2 (2010): 159-169.

[39] Hayat, T., M. Waqas, Sabir Ali Shehzad, and A. Alsaedi. "Mixed convection flow of viscoelastic nanofluid by a cylinder with variable thermal conductivity and heat source/sink." *International Journal of Numerical Methods for Heat & Fluid Flow* (2016). https://doi.org/10.1108/HFF-02-2015-0053
[40] Wang, C. Y. "Liquid film sprayed on a stretching cylinder." *Chemical Engineering Communications* 193, no. 7 (2006): 869-878. https://doi.org/10.1080/00986440500267352
[41] Mohamed, Muhammad Khairul Anuar, Siti Hanani Mat Yasin, Mohd Zuki Salleh, and Hamzeh Taha Alkasasbeh. "MHD Stagnation Point Flow and Heat Transfer Over a Stretching Sheet in a Blood-Based Casson Ferrofluid with Newtonian Heating." *Journal of Advanced Research in Fluid Mechanics and Thermal Sciences* 82, no. 1 (2021): 1-11. https://doi.org/10.37934/arfmts.82.1.111
[42] Zokri, Syazwani Mohd, Nur Syamilah Arifin, Abdul Rahman Mohd Kasim, and Mohd Zuki Salleh. "Flow of jeffrey fluid over a horizontal circular cylinder with suspended nanoparticles and viscous dissipation effect: Buongiorno model." *CFD Letters* 12, no. 11 (2020): 1-13. https://doi.org/10.37934/cfdl.12.11.113
[43] Mat, Nor Azian Aini, Norihan Md Arifin, Roslinda Nazar, and Norfifah Bachok. "Boundary layer stagnation-point slip flow and heat transfer towards a shrinking/stretching cylinder over a permeable surface." *Applied Mathematics* 6, no. 03 (2015): 466. https://doi.org/10.4236/am.2015.63044
[44] Liao, Shi-Jun. "The proposed homotopy analysis technique for the solution of nonlinear problems." *PhD diss., Ph. D. Thesis, Shanghai Jiao Tong University*, 1992.
[45] Liao, S. "An explicit, totally analytical approximate solution for Blasius equation [J]." *Int. J. Non-Linear Mech* 34 (1999): 759-778. https://doi.org/10.1016/S0020-7462(98)00056-0
[46] Liao, Shijun. *Beyond perturbation: introduction to the homotopy analysis method*. CRC press, 2003.
[47] Rashidi, Mohammad Mehdi, Abdul Majid Siddiqui, and Mostafa Asadi. "Application of homotopy analysis method to the unsteady squeezing flow of a second-grade fluid between circular plates." *Mathematical Problems in Engineering* 2010 (2010). https://doi.org/10.1155/2010/706840
[48] Usman, Auwalu Hamisu, Noor Saeed Khan, Humphries, Usa Wannasingha, Zahir Shah, Poom Kumam, Waris Khan, Amir Khan, Sadiya Ali Rano, and Zafar Ullah. "Development of dynamic model and analytical analysis for the diffusion of different species in non-Newtonian nanofluid swirling flow." *Frontiers in Physics* 8 (2021): 616790. https://doi.org/10.3389/fphy.2020.616790
[49] Shah, Zahir, Taza Gul, A. M. Khan, Ishtiaq Ali, Saeed Islam, and Fawad Hussain. "Effects of hall current on steady three-dimensional non-newtonian nanofluid in a rotating frame with brownian motion and thermophoresis effects." *Journal of Engineering Technology* 6, no. 280 (2017): e296.